Catalysis Letters Vol. 88, Nos. 3–4, June 2003 (© 2003)

Reactivity of hydroxyl species from coadsorption of oxygen and water on Ni(110) single-crystal surfaces

Hansheng Guo and Francisco Zaera*
Department of Chemistry, University of California, Riverside, CA 92521, USA

Received 27 January 2003; accepted 27 March 2003

The formation and reactivity of hydroxyl species originating from coadsorption of water and oxygen on Ni(110) single-crystal surfaces have been studied by using temperature-programmed desorption (TPD) and X-ray photoelectron spectroscopy (XPS). The resulting surface population of hydroxyl intermediates at a given water–oxygen coverage combination was found to be temperature-dependent. This was demonstrated by the differences in hydroxyl coverages determined by TPD and XPS: while the TPD data were determined to mostly reflect the maximum coverages that can be reached for a given set of gas exposures at low temperatures, the XPS results measure the OH coverages formed at the temperature of dosing. Our results indicate that, besides the stoichiometric and reversible $H_2O(ads) + O(ads) = 2\ OH(ads)$ step, a second water-decomposition reaction on the oxygen-precovered surface deposits additional hydroxyl adsorbates. Depletion of surface oxygen can be induced by thermal reaction with coadsorbed ammonia as well, a result that provides direct evidence for the OH(ads) disproportionation reaction.

KEY WORDS: surface hydroxyl groups; oxygen; water; nickel; single-crystal surfaces; thermal chemistry.

1. Introduction

Hydroxyl species are often formed on metal surfaces as the result of oxydehydrogenation [1] or hydrogen-abstraction [2] reactions between coadsorbed oxygen and hydrogen-containing molecules such as H_2O, NH_3, and alcohols. Temperature-programmed desorption (TPD) data from water and oxygen coadsorbed on Ni(110) showed that the hydroxyl yield in these systems depends critically on oxygen predoses [3]. However, a detailed examination of the parameters that affect the formation and evolution of hydroxyl species on metal surfaces has not yet been performed. As hydroxyl species are key participants in catalysis, affecting the surface chemistry of molecules such as CO [4], NH_3 [5], alkyls [6,7], alcohols [8–10], and others [11], a quantitative evaluation of the production of hydroxyl species under given water–oxygen combinations is central to the understanding of many catalytic processes.

Previous reports have indicated that the formation and subsequent conversion of OH groups from reactions of water and oxygen on Ni(110) follow a different behavior than that seen in other metals such as Ag(110). High-resolution electron energy-loss spectroscopy (HREELS) studies showed an almost quantitative reaction between H_2O and O adsorbates on Ag(110) to produce OH groups [12]. For instance, they indicated that water reacts stoichiometrically with the Ag(110)–(2 × 1)-O surface at 225 K to produce a pure (1 × 1)-OH phase. Moreover, it was also shown that heating this OH-terminated silver surface to 320 K in ultrahigh vacuum (UHV) recovers the (2 × 1)-O surface without any changes in oxygen coverage. A reversible conversion has been observed on Ni(110) by low-energy electron diffraction (LEED) between the $(3 \times 1)_i$-O ($\theta_O \sim 0.33$ ml oxygen) and (2 × 1)-OH phases when oxygen is coadsorbed with water at 300 K but, in contrast with the Ag(110) case, the reaction is clearly not stoichiometric on this nickel surface, and some water desorbs around 355 K [2]. Furthermore, a sharp LEED pattern for the Ni(110)–(2 × 1)-OH surface can only be attained after the formation of a precursor Ni(110)–$(3 \times 1)_i$-O phase, by exposing that phase to water at a constant pressure of 5×10^{-9} torr and temperatures just below 360 K [13]. The (2 × 1)-OH rectangular lattice formed under these conditions has been confirmed by time-of-flight ion scattering and recoiling spectroscopy [13].

Further reports state that water adsorption on oxygen-precovered Ni(110) surfaces between 300 and 350 K is possible only if there are unoccupied Ni(110) sites in the neighborhood of the adsorbed oxygen atoms [2]. Moreover, it is claimed that such adsorption leads to an immediate conversion to hydroxyl species. On the other hand, it has been noted from electron stimulated H^+ ion desorption angular distribution (ESDIAD) studies that abstraction of hydrogen in water coadsorbed with oxygen on these Ni(110) surfaces is facile at low temperatures [3]. Specifically, the appearance of two spots in the [001] and [00$\bar{1}$] azimuthal directions indicates the direct formation of some OH(ads) upon adsorption of fractional monolayers of H_2O on O/Ni(110) at 80 K, though effective conversion of H_2O to OH only occurs at temperatures between 200 and 270 K, in competition with molecular water desorption [3]. The

---

* To whom correspondence should be addressed.

1011-372X/03/0600–0095/0 © 2003 Plenum Publishing Corporation

maximum reactivity of the surface oxygen with coadsorbed water appears to occur at oxygen coverages around 0.15 ml, significantly lower to those needed for the formation of the $(3 \times 1)_i$-O phase [13], but the exact conditions that optimize hydroxyl formation have not yet been identified.

In this work, a systematic study was carried out on the extent of water decomposition and hydroxyl formation on Ni(110) surfaces as a function of atomic oxygen and water coverages. The surface populations of the hydroxyl species were estimated by both XPS and TPD. These two techniques provide quite complementary information. On the one hand, since hydrogen-abstraction and hydroxyl disproportionation reactions reach their highest rates at different temperatures, and since in the water–oxygen coadsorbed system the surface OH population changes with surface temperature, the TPD data only represents the overall OH surface coverages formed at the low temperatures of water deposition. On the other hand, XPS provides the OH population formed at a given water-adsorption temperature. By comparison of the TPD and XPS data, the evolution of the OH groups as a function of temperature was characterized, and with that information an inference on the key sites on the oxygen-predosed Ni(110) needed for abstraction of hydrogen in H_2O was made.

2. Experimental

The experiments reported here were conducted in an UHV system equipped with instrumentation for TPD, XPS, and LEED. Details of the system have been provided previously [14–16]. The base pressure of the system was approximately 2×10^{-10} Torr. TPD experiments were carried out with a UTI quadruple-mass spectrometer equipped with a front retractable cone for selective probing of the gases desorbing from the front face of the crystal and interfaced to a personal computer. XPS data were taken by using a 100-mm concentric hemispheric analyzer combined with a dual X-ray source from Vacuum Generators Corp.

A Ni(110) single-crystal disk, 10 mm in diameter and 1.0 mm in thickness, was used as the substrate after polishing of the front face. Ta-wires of diameter 0.5 mm were spot-welded to the edge of the crystal and fixed on the ends of two copper posts connected to a liquid nitrogen reservoir via vacuum feedthroughs. This setup allowed for cooling of the sample down to 90 K and for its resistive heating to up to 1100 K. A K-type thermocouple was spot-welded to the edge of the crystal to monitor its temperature, and a homemade temperature controller was used to provide linear temperature ramps or to maintain the crystal within ±0.5 K of a given temperature value. A heating rate of 10 K s^{-1} was used for the TPD measurements. The Ni(110) crystal was cleaned by repeated cycles of Ar^+ ion sputtering and annealing until a clean and well-ordered surface was obtained, as determined by XPS and CO TPD experiments.

Dioxygen and ammonia (> 99.998%) were purchased from Matheson and used as supplied. Regular deionized water was used after several freeze–pump–thaw cycles. All gases were dosed by raising the ambient pressure using individual leak vales for each compound. Pressures were measured by using a nude ion gauge, not calibrated for differences in ion-gauge sensitivities. Oxygen dosing was always performed at 400 K to ensure dissociative adsorption [3,17], while water was adsorbed at different temperatures as indicated throughout the text. Damage by stray electrons was minimized by biasing of the sample all throughout the TPD experiments.

Water coverages were calibrated using appropriate TPD spectra. The total TPD intensity of adsorbed water dosed on clean Ni(110) at 120 K displays a linear relation versus dose up to 3.0 l, the maximum exposure used in these experiments. It was found that 1.0 l water exposures at 120 K saturate the chemisorption peaks, which have been determined to correspond to approximately 0.50 monolayers ($1\,\text{ml} = 1.14 \times 10^{15}$ molecules cm^{-2}) [18]. For the case of water uptake on oxygen-predosed surfaces (typically $\theta_O = 0.15\,\text{ml}$), the total TPD intensity of the desorbing water also displays a linear dependence on exposure, but with a slightly lower slope, so that 1.0 l H_2O exposures correspond to approximately $\theta_{H_2O} = 0.46\,\text{ml}$. This difference may be attributed to the result of some water decomposition on the oxygen-treated surface [3].

Oxygen adsorbs dissociatively on the Ni(110) surface, with a near constant sticking coefficient at low exposures and surface temperatures between 300 and 500 K [3,14]. This was properly used to estimate oxygen coverages for O_2 exposures below 0.3 l, that is, before the formation of the 0.3 ml $(3 \times 1)_i$-O structure. However, the linearity between exposure and coverage for oxygen breaks down above 0.3 l: a (2×1)-O pattern can only be effectively produced at oxygen exposures around 1.0 l (and surface temperatures above 300 K) [3]. This effect was also taken into account when designing our experiments.

3. Results and Discussion

3.1. Water decomposition on oxygen-precovered Ni(110) surfaces

Our work on the adsorption of water on clean Ni(110) surfaces agrees well with previous TPD, FTIR, LEED, and ESDIAD studies [18,19]. Figure 1(a) shows the H_2 and H_2O TPD spectra obtained from 1.0, 2.0, and 3.0 l of water dosed on Ni(110) at 120 K. The water desorption peaks seen in those traces have been assigned to ice layers (180 K, C), hexagonal H_2O clusters

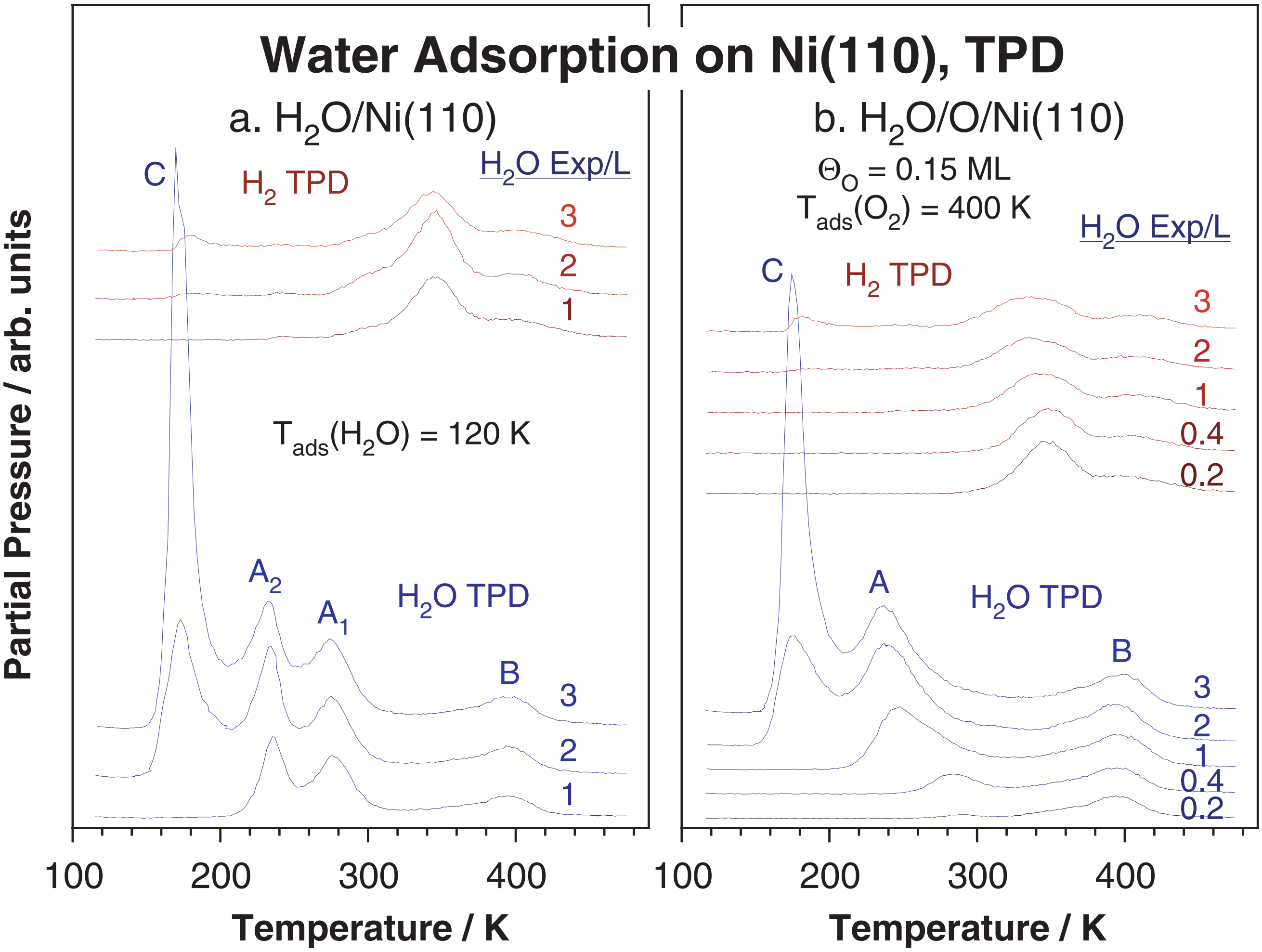

Figure 1. Temperature-programmed desorption (TPD) spectra for H_2O and H_2 from Ni(110) surfaces dosed with (a) water alone and (b) after oxygen exposures. The water was dosed at 120 K in all cases, and 0.15 ml of oxygen was predeposited in the second (b) case at 400 K. Significant changes are observed upon oxygen preadsorption, indicating an enhanced yield in the OH-disproportionation (B) feature and the merging of the two water monolayer molecular desorption (A_1 and A_2) peaks into a single (A) desorption state.

(230 K, A_2), H_2O dimers (280 K, A_1), and disproportionation of OH(ads) groups arising from previous partial dissociation of H_2O (400 K, B) [3]. These adsorption states are populated in the reverse order so that they desorb during the TPD experiments, that is, the $A_1 + B$ states grow first, then the A_2 state, and finally the C peak. Most of the hydrogen desorption is observed around 340 K, but there are additional features at about 300 and 400 K.

Previous studies also showed that the maximum reactivity of water with predosed oxygen occurs at around $\theta_O = 0.15$ ml, as indicated by a maximum in yield for the H_2O TPD peak corresponding to the disproportionation of water (the B peak) [3,5]. In the experiments reported in figure 1(b), 0.15 ml of oxygen and varying amounts of water were adsorbed successively at 400 and 120 K, respectively, to produce OH groups on the Ni(110) surface. Comparison of figures 1(a) and 1(b) indicates that the most obvious changes induced on the surface chemistry of adsorbed water by the predosed oxygen are the merging of the A_1 and A_2 chemisorption states into a single A desorption state around 240 K [3], and the enhancement of the OH-disproportionation B peak. The growth of peak B, in particular, is easily attributed to the formation of additional OH(ads) via a new reaction pathway between H_2O(ads) and O(ads) [2].

On O/Ni(110) surfaces, the water-adsorption states are populated in the same order as on the clean surface, in particular, the B state is populated first, but the A state starts to grow before the B state reaches saturation. The TPD spectra in figure 1(b) also show that the desorption temperatures for water from the B and C states are independent of water coverage, but that the desorption temperature of the A state shifts monotonically down with coverage. On clean Ni(110), the chemisorbed water molecules initially combine into dimers (A_1 states) but then grow into hexagonal clusters (A_2) with increasing water coverage; each A_1 and A_2 state gives rise to distinct and characteristic desorption peaks (as seen in figure 1(a)) [3]. On the oxygen-precovered Ni(110) surface, on the other hand, the adsorbed water no longer forms distinct dimer and/or hexagonal groups, but preferentially clusters around the oxygen surface atoms instead, and, thanks to the stabilization of the adjacent water molecules induced by the oxygen adsorbates [20], desorbs at higher temperatures than on the clean nickel, at least at low coverages (see the A peaks at water exposures below 0.4 l). It can be suggested that the size of the water clusters increases as the water coverage is increased and that the shifts observed in the A peak with H_2O dose are caused by an increase of the in-plane repulsive interaction among the water adsorbates with increasing average cluster size. Once the first layer of water is saturated (~1.0 l, or ~0.5 ml), the A peak reaches its final desorption temperature and intensity, and is not affected by the piling up of additional water, leading to the growth of the C TPD feature during condensation.

The H_2 TPD spectra displayed in figure 1 provide additional information on the effect of adsorbed oxygen on the chemistry of water on Ni(110) surfaces. The H_2 yields (in unit of ml) as a function of water coverage are reported in figure 2(a). These yields were estimated from the areas under the TPD peaks, without the feature around 180 K (which corresponds to cracking of the C state of water in the mass spectrometer), after calibration using the atomic O 1s XPS intensity due to water decomposition on the clean surface. We found that when 1.0 ml of water is deposited on clean Ni(110) at 120 K and then heated to 475 K (to completely drive the disproportionation of OH species), about 0.08 ml of atomic oxygen remains on the surface (data not shown), in agreement with previously reported AES measurements on the same system [3]. This residual oxygen corresponds to ~0.16 ml of H(ads) from water decomposition. According to the data in figure 2(a), H_2 desorption from H_2O adsorbed on clean Ni(110) reaches a maximum yield around 2.0 l H_2O exposures (~1 ml coverage), and decreases afterwards, so that at 3.0 l it is reduced to the same value as that for 1.0 l. Predosed oxygen significantly reduces the total H_2 yield compared to that from the same H_2O exposures without oxygen predose, suggesting that hydrogen transfer to the adsorbed oxygen to produce OH surface species may inhibit some of the alternative H_2O decomposition pathway to $H_2(g) + O(ads)$. Also, the H_2 desorption peak at 350 K tends to broaden on the low-temperature side with increasing water exposure, perhaps because the resulting higher OH(ads) coverages weaken the adsorption energy of a fraction of the H(ads) surface species produced by water dehydrogenation.

Figure 2(b) displays both the total water yield and the contribution from the OH-disproportionation pathway as a function of water coverage for the case of a 0.15-ml oxygen predose. It can be seen here that for H_2O exposures below 0.15 l the adsorbed water converts completely into surface OH groups. Above 0.15-l H_2O, on the other hand, the total TPD water intensity keeps increasing in a linear fashion, but the contribution from disproportionation of OH species slowly approaches a limiting water yield of ~0.2 ml. Similar behavior has been reported earlier for the $D_2O/O(0.2\,ml)/Ni(110)$ system [4]. Since two OH surface groups are required to yield one desorbing water molecule in the B H_2O TPD state $(2\,OH(ads) \rightarrow H_2O\uparrow + O(ads))$, the maximum OH coverage possible in this case is approximately 0.4 ml.

The water yields from OH disproportionation estimated by TPD experiments are shown in figure 3 as function of water exposure at 300 K for Ni(110) surfaces predosed with 0.1 ml and 0.2 ml of oxygen. The H_2O yield from this reaction increases monotonically with water dose up to approximately 1.0 ml for both the oxygen coverages. However, the water yields for the case of the 0.2 ml oxygen predose are far lower than twice the corresponding intensities in the 0.1 ml case. This acute nonlinearity in OH-disproportionation yield with oxygen coverage indicates that by 0.2 ml oxygen predoses the resulting surface is not as efficient in converting atomic oxygen into hydroxyl species as that with the lower oxygen coverages. This change can be understood in terms of the –Ni–O– chain/island growth that takes place on Ni(110) upon oxygen exposures above 400 K [3,17]: the $H_2O(ads) + O(ads) \rightarrow 2\,OH(ads)$ conversion is likely to occur at the end of those –Ni–O– chains, so the remaining O(ads) may not be able to readily hydrogenate to form surface hydroxyl groups. Oxygen uptakes above 0.1 ml may mostly contribute to an increase in the size of the existing rows rather than to the creation of new –Ni–O– islands, so the relative fraction of edge oxygen sites may decrease with coverage.

The higher reactivity of the oxygen adsorbates at the –Ni–O– chain ends has been confirmed by STM in H_2-titration studies of the Ni(110)–$(3 \times 1)_f$-O surface ($\theta_O \approx 0.67$ ml, with two added rows for every three $[1\bar{1}0]$ lattice spacings [21]) at 470 K. Only about 2% of the oxygen on large terraces can be removed in those experiments after 100 l H_2 exposures, even though essentially all oxygen can be titrated from the higher step density regions with much lower H_2 exposures [22]. In fact, the story is complicated further by the fact that the –Ni–O– strings become mobile on the Ni(110) surface at temperatures above 350 K, more so in the presence of adsorbates such as oxygen, water, or hydrogen. It is this dynamic process that enabled Roux *et al.* to attain a well-ordered Ni(110)–(2×1)-OH surface by exposing the Ni(110)–$(3 \times 1)_i$-O to water at just below 360 K, the initial temperature of OH disproportionation [13].

3.2. Temperature dependence of the OH(ads) population

The production of water from OH disproportionation was also studied as a function of H_2O dosing temperature. In the TPD experiments reported in figure

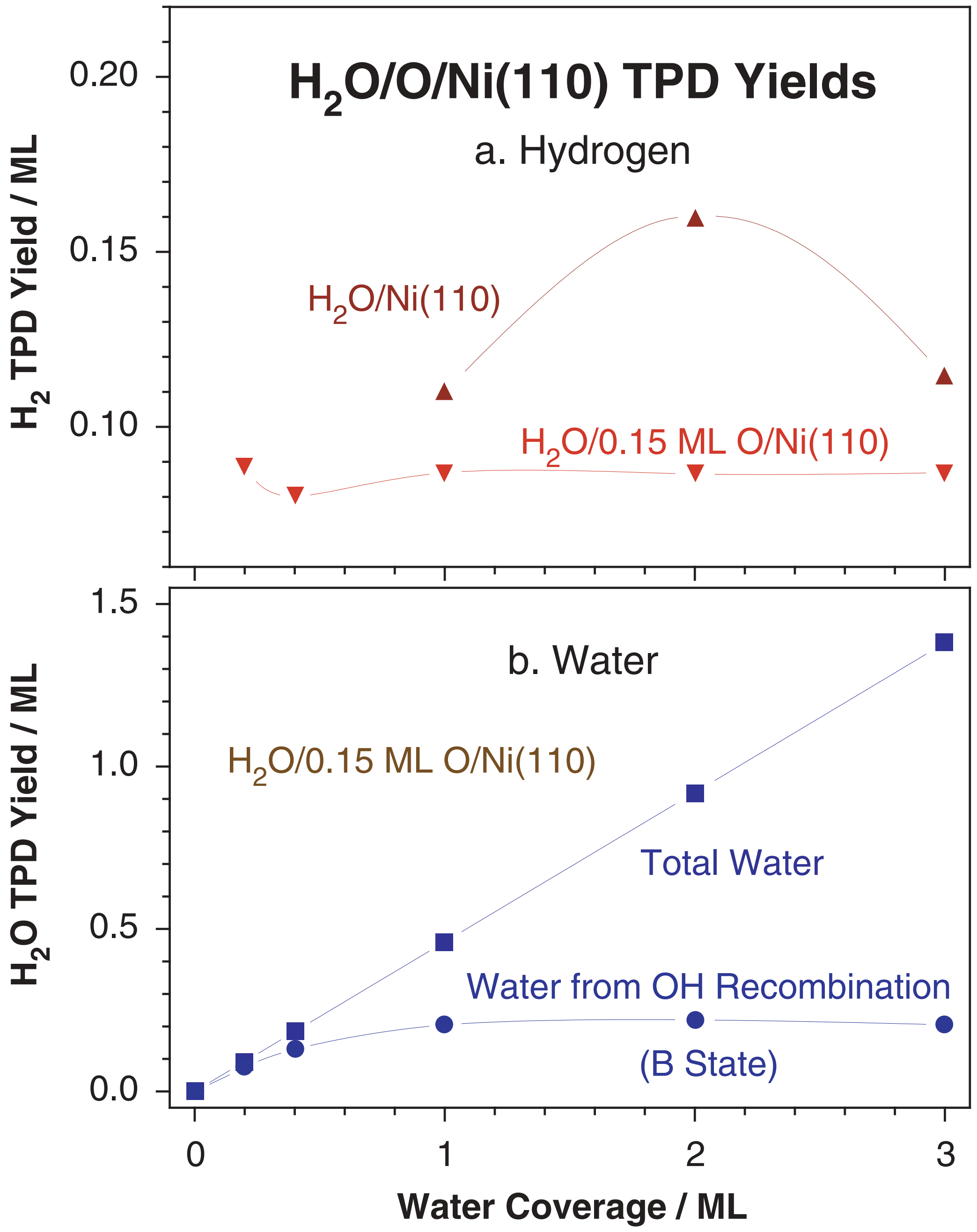

Figure 2. (a) H_2 TPD yields from water dosed on clean and oxygen-predosed Ni(110) surfaces as a function of H_2O exposure. (b) TPD yields for the overall water desorption and for the water produced by OH disproportionation for the $H_2O + O$ coadsorption system. Water was dosed at 120 K in all cases, and a $\theta_O = 0.15$ ml coverage was used for the experiments with O/Ni(110) (prepared by dosing O_2 at 400 K). Clearly, oxygen inhibits the total dehydrogenation of adsorbed water into O(ads) + 2 H(ads).

4(a), the coverage of oxygen was kept at 0.2 ml, and the water exposure was chosen at 0.2 ml to saturate the OH recombination H_2O TPD state around 400 K (B) while minimizing the filling of the chemisorption (A) water states (although a little signal for peak A can still be seen at 280 K in most of the spectra). According to these data, the yields for both chemisorbed water and OH disproportionation are approximately constant, but are slightly higher for the case of water exposure at lower temperatures (120 K). Figure 4(b) displays the corresponding O 1s XP spectra for the cases of water dosing at 120, 200, 250, and 300 K. The data were deconvoluted by assuming the existence of three surface species, namely, H_2O, OH, and atomic oxygen, as identified in the past [23,24]. Nonlinear least-squares fitting was performed for all four traces in figure 4(b) by using Gaussian functions and by fitting the peak energy and width values appropriately; three components were identified this way with binding energies centered at 532.6, 531.2, and 530.1 eV, respectively. The spectra in

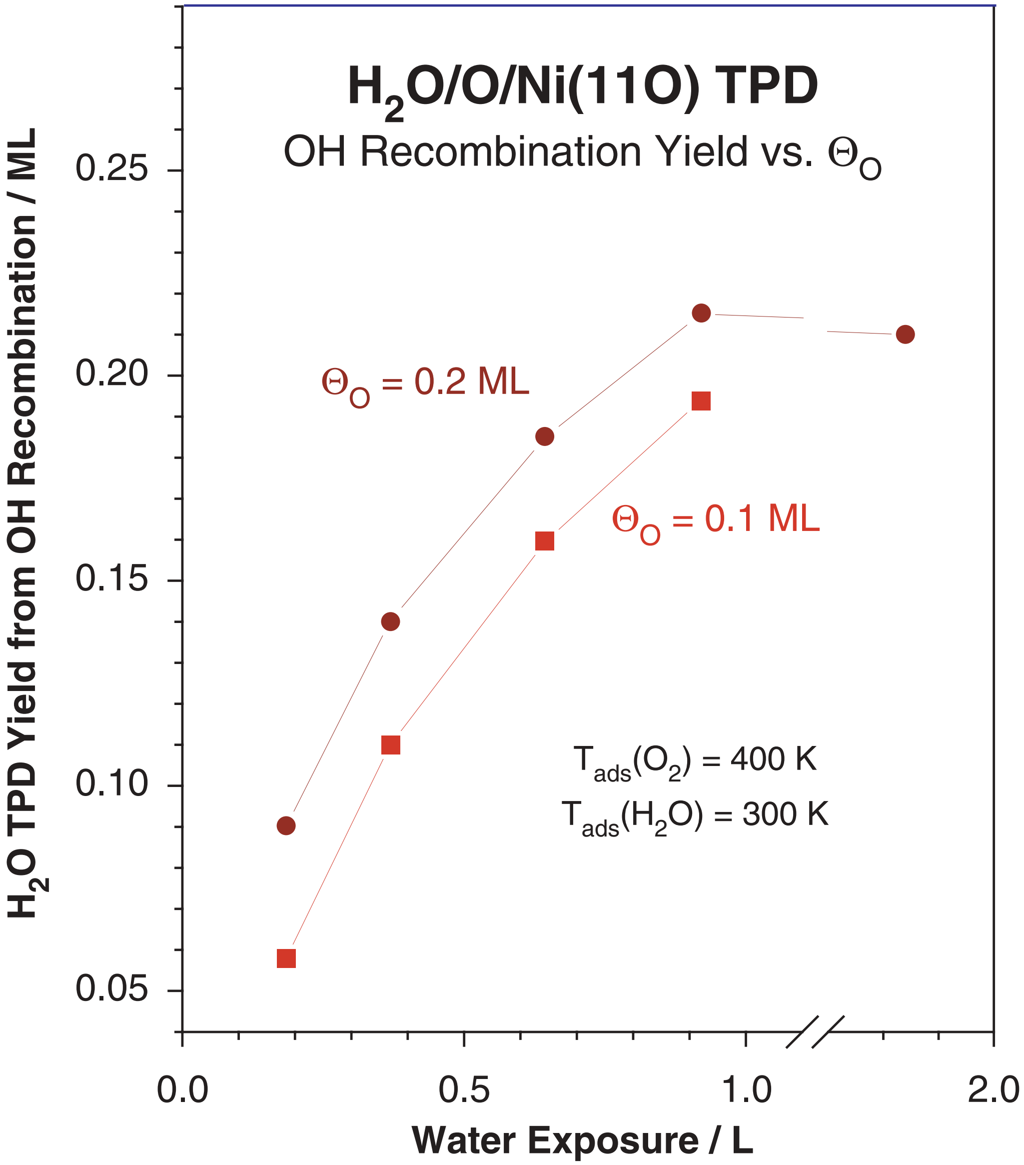

Figure 3. Dependence of the TPD water yield from OH disproportionation on H_2O exposure for two different oxygen predoses. In these experiments, water was adsorbed on the surface at 300 K to minimize molecular adsorption. It is noted that the water yields for the case of the 0.2 ml oxygen predose does not correspond to twice the intensity of the 0.1 ml case. This suggests that the $H_2O(ads) + O(ads) \rightarrow 2\ OH(ads)$ conversion occurs preferentially at the end of the –Ni–O– chains formed by oxygen adsorption on Ni(110).

figure 4(b) indicate that the relative intensity of the OH component (at 531.2 eV) increases with increasing deposition temperature. It should be noted that, as these spectra were acquired during 20-min intervals each at 120 K, the molecular water component (the shoulder at higher binding energy) may contain a significant contribution from water readsorption from residual gases.

The temperature dependence of the conversion of the coadsorbed oxygen and water into OH groups for H_2O(0.2 l)/O(0.2 ml)/Ni(110) is depicted quantitatively in figure 5. There, OH surface coverages, obtained independently by integration of the TPD traces in figure 4(a) and the O 1s XPS peak for OH(ads) in figure 4(b), are reported, after calibration via the matching of the TPD and XPS data at 300 K. The results in figure 5 indicate that the OH coverages derived by TPD and XPS display opposite trends: while the amount of OH that converts to water in the TPD experiments is maximum for water adsorption at 120 K (0.183 ml), the surface concentration of OH species measured by XPS reaches the highest intensity at 300 K (0.150 ml). This discrepancy is explained by the fact that, while the XPS data provide a direct measure of the OH coverage at the deposition temperature, the TPD signal corresponds to the total OH intermediates available above ~350 K, the temperature of the OH disproportionation. By comparison of the TPD and XPS values, specifically

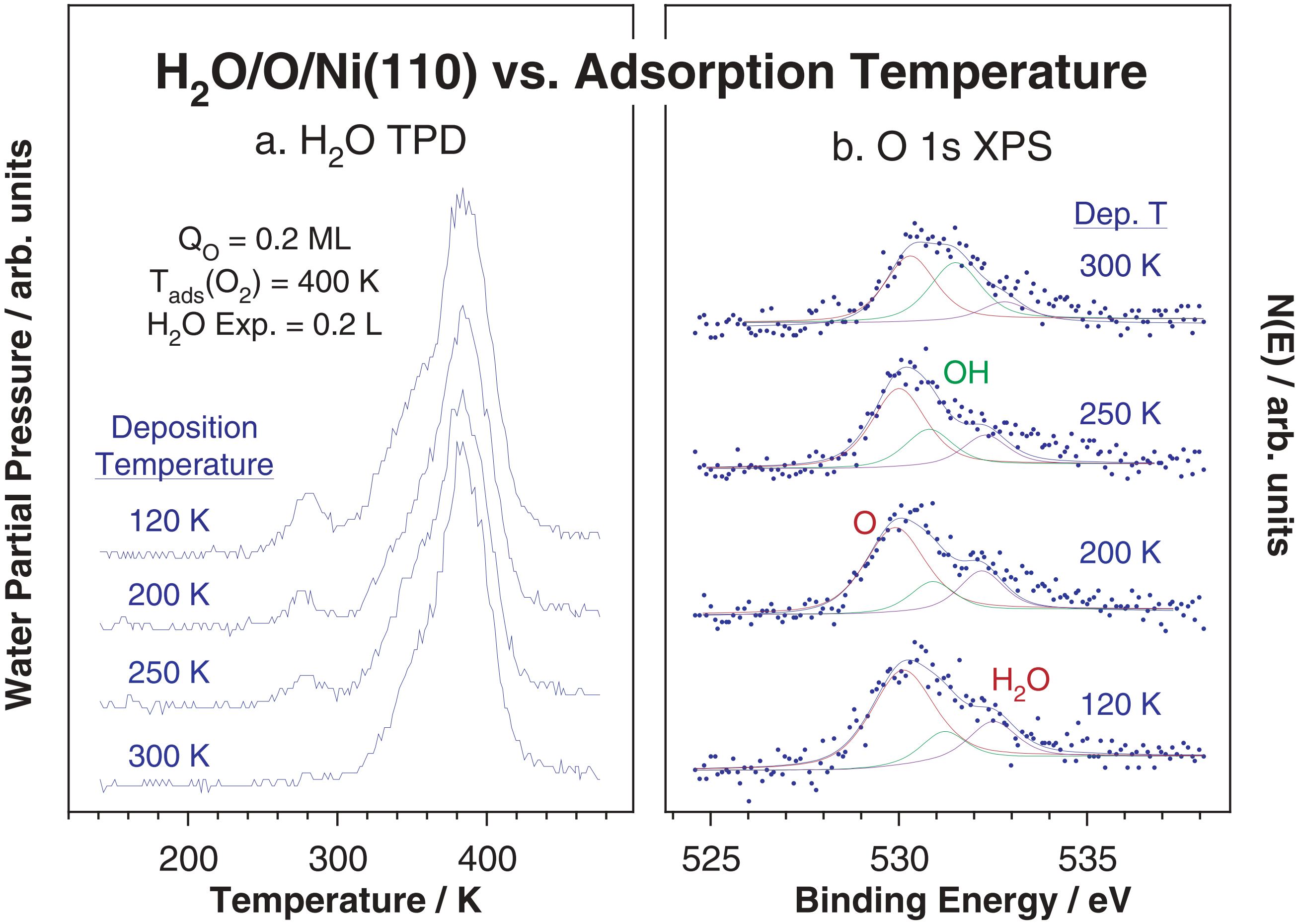

Figure 4. (a) Water TPD traces from $H_2O(0.2 l)/O(0.15 ml)/Ni(110)$ as a function of water deposition temperature. Minor amounts of molecular water desorption were detected when water was deposited at 120, 200, and 250 K, but the main component at 390 K, owing to OH disproportionation, varies little with deposition temperature. (b) Corresponding O 1s XP spectra. These data were fitted to three peaks associated with H_2O, OH, and atomic oxygen surface species. The H_2O components in the spectra may include a contribution from readsorption of water from residual gases.

at 120 K, these apparently contradictory results in fact indicate that only a fraction (about a third) of the OH species from reactions between coadsorbed H_2O and O are produced at low adsorption temperatures [19] and that additional OH groups (~0.12 ml, the remaining two-thirds) are produced as the surface temperature is ramped during the TPD experiments.

Figure 5 also indicates that the total yield of OH groups in TPD experiments does not depend strongly on the initial temperature of adsorption. The small difference in the total OH yield seen between the cases of water adsorption at 120 and 300 K (~0.03 ml) may be attributed to different reaction pathways. At 300 K, the adsorbing water converts directly into OH groups by reaction with surface oxygen, otherwise it would not be retained on the surface [2]. On the other hand, at 120 K, stable H_2O–O clusters are likely to form on the surface and react at different temperatures depending on their size.

3.3. *Production and consumption of surface O(ads) when coadsorbed with water*

It has so far been established that oxygen and water coadsorbed on Ni(110) surfaces follow the reversible reaction:

$$H_2O(ads) + O(ads) \rightarrow 2\ OH(ads) \qquad T < 300\,K \quad (1)$$

$$2\ OH(ads) \rightarrow H_2O \uparrow + O(ads) \qquad T \geq 300\,K \quad (2)$$

However, the (1)–(2) adsorption–desorption cycle leads to a H_2O TPD yield a little lower than that expected from the amount of water initially dosed on the surface. This is due to total dehydrogenation of some of the adsorbed water, a reaction promoted by oxygen adsorbates. Actually, a small amount of water can decompose even on clean Ni(110) surfaces [25], as evidenced by the steady appearance of the H_2 peaks in the TPD spectra in figure 1(a). The decomposition of

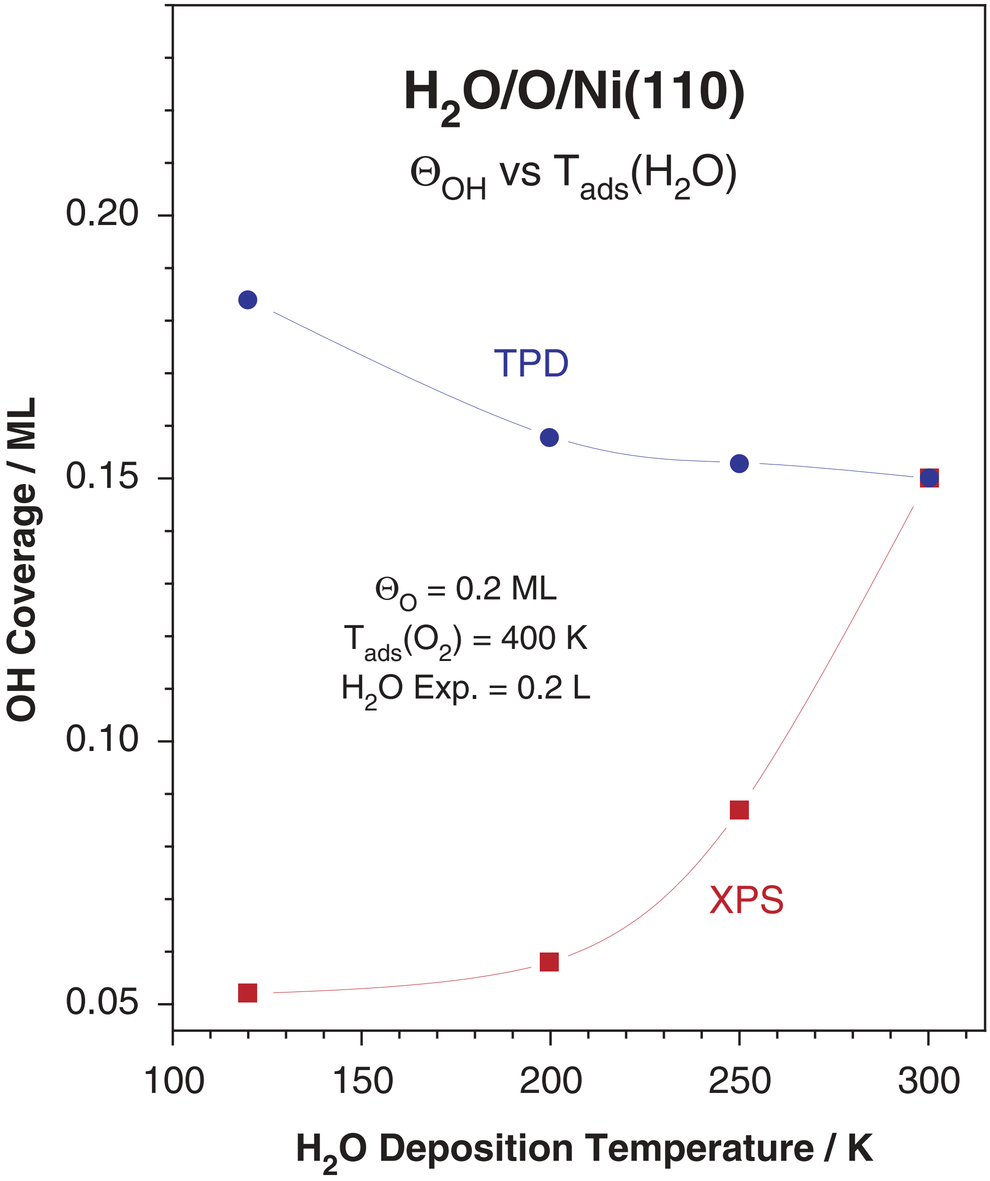

Figure 5. OH coverages, in monolayers, for the H_2O(0.2 l)/O(0.2 ml)/Ni(110) system as a function of water deposition temperature. The XPS results represent the OH coverage formed at the temperature of water exposure, while the TPD data corresponds to the maximum OH coverages produced in the TPD experiments. The same OH coverages from water deposition at 300 K were assumed for both TPD and XPS experiments.

water in that case may be catalyzed by a minor amount of residual oxygen ($\leq$ 0.01 ml) that may remain on the Ni(110) surface [25], but it may also be aided by structural defect sites on that single-crystal surface such as steps or kinks. On the other hand, adsorbed oxygen on the Ni(110) surface promotes the dissociation of water to form OH intermediates, as shown in figure 1(b) and quantitatively in figure 2(b). Indeed, the OH yields reach a value of ~0.4 ml for a combination of 0.15 ml O(ads) and 1.0 l water exposure, surpassing the conversion yield expected from a $H_2O + O$ stoichiometric reaction (in which 0.3 ml OH(ads) is expected, the rest of the water desorbing molecularly). The production of H_2 and the increase in the B-water yield (from disproportionation of OH intermediates) indicate that additional oxygen is produced on the surface in the water–oxygen coadsorption system upon heating above room temperature.

In order to better follow the fate of the preadsorbed oxygen during its reaction with water, analogous experiments were carried out with ammonia [5]. These experiments also served to confirm the nature of the disproportionation reaction of the OH surface groups. A direct consequence from OH disproportionation is the depletion of the total surface oxygen coverage, as water desorbs into the gas phase. It has been previously shown that ammonia and water follow similar H-transfer chemistry on oxygen-predosed metal surfaces [16], except that with ammonia the formation of OH groups on the oxygen-predosed Ni(110) takes place by the

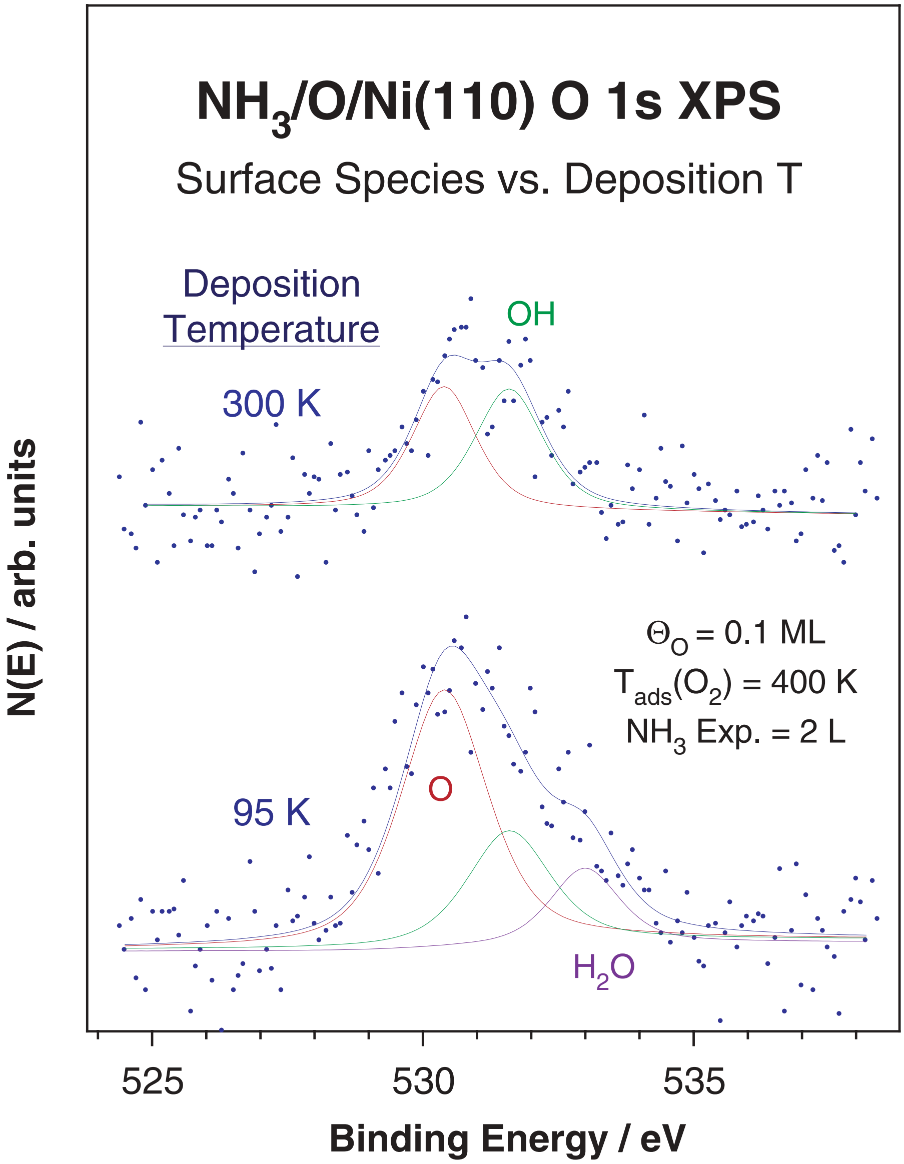

Figure 6. O 1s XP spectra from ammonia coadsorbed with oxygen on a Ni(110) surface. First oxygen was adsorbed at 400 K, then ammonia was dosed at 95 K (lower spectrum) and 300 K (upper spectrum). The desorption of water from disproportionation of OH groups made by $NH_3(ads) + O(ads)$ reactions explains the significant depletion of the O(ads) signal seen at 300 K.

analogous to Reaction (1):

$$NH_3(ads) + O(ads) \rightarrow OH(ads) + NH_2(ads)\ T < 300\,K \tag{3}$$

At higher temperatures, reaction (2), the disproportionation of the OH(ads) groups, is still possible. Figure 6 displays two O 1s XP spectra from the NH_3(2 l)/O(0.1 ml)/Ni(110) system, where the NH_3 was dosed at 95 K (lower spectrum) and 300 K (upper spectrum). It is seen from these experiments that, indeed, about half of the initial surface oxygen is removed by the formation and desorption of water when ammonia is dosed at 300 K. The hydroxyl and water components observed in the 95 K spectrum may originate from direct hydrogen transfer from the coadsorbed ammonia to O(ads), a step that, again, is supposed to preferentially occur at the end of the –Ni–O– rows. Notice also that some OH(ads) groups are still present on the surface at 300 K.

4. Conclusions

The chemistry of water and oxygen coadsorbed on Ni(110) can be characterized as follows:

(1) Oxygen predosed on Ni(110) can significantly modify the nature of the adsorption states of water on that surface. Instead of the formation of the dimers and hexagonal clusters seen on clean nickel, water aggregates preferentially at the perimeter of oxygen adsorbates instead. The continuous growth

of these oxygen-seeded water clusters in the first layer presumably increases the repulsive interaction among the chemisorbed water molecules, and results in a continuous shift of the chemisorption (A) H_2O TPD peak toward lower temperatures with increasing H_2O dose.

(2) Adsorbed water reacts readily with surface oxygen atoms to form hydroxyl species. This reaction is already seen at low temperatures, presumably because of the facile nature of the hydrogen transferring at the end of –Ni–O– rows. However, for the specific case of $H_2O(0.2\,l)/O(0.2\,ml)/$ Ni(110), only about a third of the OH species forms at 120 K, while the rest is produced slowly as the temperature of the surface is increased. This temperature-dependent slow conversion is probably associated with the different sizes of the H_2O–O(ads) clusters that form on the surface. Complete conversion is only possible at water exposures below 0.15 l and low oxygen coverages ($\theta_O \leq 0.15\,ml$).

(3) The stoichiometric and reversible oxygen-assisted water-decomposition reaction, $H_2O(ads) + O(ads) = 2\ OH(ads)$, is accompanied by some additional total dehydrogenation of water on the oxygen-precovered Ni(110) surface. The latter process results in the production of H_2 in TPD experiments, and is also manifested by an increase in the coverage of O(ads) species above 300 K, as indicated by O 1s XP spectra. More extensive dehydrogenation is seen on the clean Ni(110) surface.

(4) OH(ads) surface groups undergo a disproportionation reaction back to adsorbed oxygen and water (the reverse of the OH production step) above ~350 K. This disproportionation step leads to the depletion of the surface concentration of O(ads), as also seen in oxygen–ammonia coadsorbed systems.

Acknowledgment

Financial support for this research was provided by the Department of Energy, Basic Energy Sciences Division, under contract DE-FG03-01ER15182.

References

[1] G.U. Kulkarni, C.N.R. Rao and M.W. Roberts, J. Phys. Chem. 99 (1995) 3310.

[2] C. Benndorf, C. Noebl and T.E. Madey, Surf. Sci. 138 (1984) 292.

[3] C. Benndorf and T.E. Madey, Surf. Sci. 194 (1988) 63.

[4] T. Yuzawa, T. Higashi, J. Kubota, J.N. Kondo, K. Domen and C. Hirose, Surf. Sci. 325 (1995) 223.

[5] H. Guo and F. Zaera, Surf. Sci. 524 (2003) 1.

[6] N.R. Gleason and F. Zaera, in *3rd World Congress on Oxidation Catalysis*, San Diego, CA, 21–26 September 1997, R.K. Grasselli, S.T. Oyama, A.M. Gaffney and J.E. Lyons (eds), *Studies in Surface Science and Catalysis Series*, Vol. 110 (Elsevier, Amsterdam, 1997) p. 235.

[7] F. Zaera, N.R. Gleason, B. Klingenberg and A.H. Ali, J. Mol. Catal., A 146 (1999) 13.

[8] V.S. Lusvardi, M.A. Barteau, W.R. Dolinger and W.E. Farneth, J. Phys. Chem. 100 (1996) 18183.

[9] F. Zaera, J.M. Guevremont and N.R. Gleason, J. Phys. Chem. B 105 (2001) 2257.

[10] F. Zaera, Catal. Today (2002); in press.

[11] J.N. Kondo, T. Yuzawa, J. Kubota, K. Domen and C. Hirose, Surf. Sci. 343 (1995) 71.

[12] M. Borbach, W. Stenzel, H. Conrad and A.M. Bradshaw, Surf. Sci. 377–379 (1997) 796.

[13] C.D. Roux, H. Bu and J.W. Rabalais, Surf. Sci. 279 (1992) 1.

[14] H. Öfner and F. Zaera, J. Phys. Chem. B 101 (1997) 9069.

[15] D. Chrysostomou, J. Flowers and F. Zaera, Surf. Sci. 439 (1999) 34.

[16] H. Guo, D. Chrysostomou, J. Flowers and F. Zaera, J. Phys. Chem. B 107 (2003) 502.

[17] L. Ruan, I. Stensgaard, E. Lægsgaard and F. Besenbacher, Surf. Sci. 314 (1994) L873.

[18] B.W. Callen, K. Griffiths, U. Memmert, D.A. Harrington, S.J. Bushby and P.R. Norton, Surf. Sci. 230 (1990) 159.

[19] B.W. Callen, K. Griffiths, R.V. Kasza, M.B. Jensen, P.A. Thiel and P.R. Norton, J. Chem. Phys. 97 (1992) 3760.

[20] K. Bange, D.E. Grider, T.E. Madey and J.K. Sass, Surf. Sci. 137 (1984) 38.

[21] L. Eierdal, F. Besenbacher, E. Laegsgaard and I. Stensgaards, Surf. Sci. 312 (1994) 31.

[22] P.T. Sprunger, Y. Okawa, F. Besenbacher, I. Stensgaard and K. Tanaka, Surf. Sci. 344 (1995) 98.

[23] G.U. Kulkarni, C.N.R. Rao and M.W. Roberts, Langmuir 11 (1995) 2572.

[24] J.C. de Jesús, J. Carrazza, P. Pereira and F. Zaera, Surf. Sci. 397 (1998) 34.

[25] B.W. Callen, K. Griffiths, P.R. Norton and D.A. Harrington, J. Phys. Chem. 96 (1992) 10905.